

# Single-Molecular Artificial Transmembrane Water Channels

Xiao-Bo Hu, Zhenxia Chen, Gangfeng Tang, Jun-Li Hou,\* and Zhan-Ting Li

Department of Chemistry, Fudan University, 220 Handan Road, Shanghai 200433, China

**S** Supporting Information

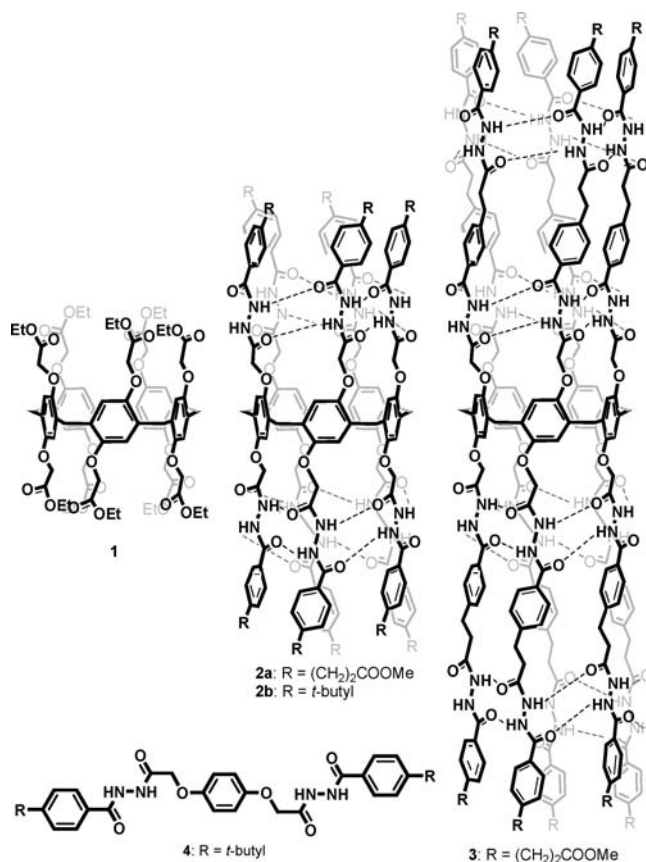
**ABSTRACT:** Hydrazide-appended pillar[5]arene derivatives have been synthesized. X-ray crystal structure analysis and  $^1\text{H}$  NMR studies revealed that the molecules adopt unique tubular conformations. Inserting the molecules into the lipid membranes of vesicles leads to the transport of water through the channels produced by single molecules, as supported by dynamic light scattering and cryo-SEM experiments. The channels exhibit the transport activity at a very low channel to lipid ratio (0.027 mol %), and a water permeability of  $8.6 \times 10^{-10} \text{ cm s}^{-1}$  is realized. In addition, like natural water channel proteins, the artificial systems also block the transport of protons.

Transmembrane water transport is crucially important for the regulation of the osmotic pressure of cells. Nature utilizes water channel proteins, called aquaporins,<sup>1</sup> to realize this purpose.<sup>2</sup> The development of synthetic systems displaying powerful water transport capability not only is fundamentally important but also may lead to the generation of new medicinal<sup>3</sup> and environmental materials, for example, for water purification.<sup>4</sup> Currently, a large number of artificial systems for transmembrane transport of ions and neutral organic solutes have been reported.<sup>5,6</sup> In contrast, although theoretical calculations have suggested that many structures can be used for transmembrane water transport,<sup>7,8</sup> the creation of mimicking systems has been a challenge because of the lack of synthetic architectures that can form long and narrow channels for water.<sup>9</sup> We were inspired to design artificial water channels by mimicking the single pore feature of natural channel proteins.<sup>10</sup> Herein we describe the first example of artificial single-molecular transmembrane water channels formed from hydrazide-appended pillar[5]arenes, which display transport activity at very low concentration.

We recently reported that pillar[5]arene derivative **1** (Chart 1) induces the formation of water wires,<sup>11</sup> which could be utilized to mediate transmembrane proton transport.<sup>12,13</sup> To exploit further the potential of such tubular systems for water transport, we prepared **2a**, **2b**, and **3** by attaching 10 hydrazide-incorporated side chains to the central pillar[5]arene scaffold (Chart 1). It was envisioned that the hydrazide units in the side chains might form pentameric cylinders through intramolecular hydrogen bonding to induce the whole molecules to produce tubular structures.<sup>14</sup>

The  $^1\text{H}$  NMR spectrum of control molecule **4** in  $\text{CDCl}_3$  (Figure 1a) displayed one set of sharp signals, and the N–H signals of the hydrazide units appeared at 9.28 and 8.67 ppm. In contrast, the spectra of **2a**, **2b**, and **3** all had lower resolution, and their N–H signals were shifted downfield (Figure 1b–d).

Chart 1. Structures of Compounds 1–4<sup>a</sup>



<sup>a</sup>The hydrazide units of **2a**, **2b**, and **3** form pentameric cylinders through intramolecular hydrogen bonding to induce the formation of tubular structures.

Diluting their solutions from 2 mM to 0.2 mM did not cause an observable change in the chemical shift of the N–H signals. The spectra recorded in deuterated dimethyl sulfoxide ( $\text{DMSO}-d_6$ ) had high resolution [see the Supporting Information (SI)]. All of these results suggested that the hydrazide units of **2a**, **2b**, and **3** were involved in intramolecular hydrogen bonding, which should induce the whole molecule to form a tubular conformation. Single crystals of **2b** suitable for X-ray crystallographic analysis were obtained by slow evaporation of its solution in 1:1 (v/v)  $\text{CHCl}_3/\text{MeOH}$ . The crystal structure revealed that eight of the 10 hydrazide groups

Received: March 8, 2012

Published: May 10, 2012

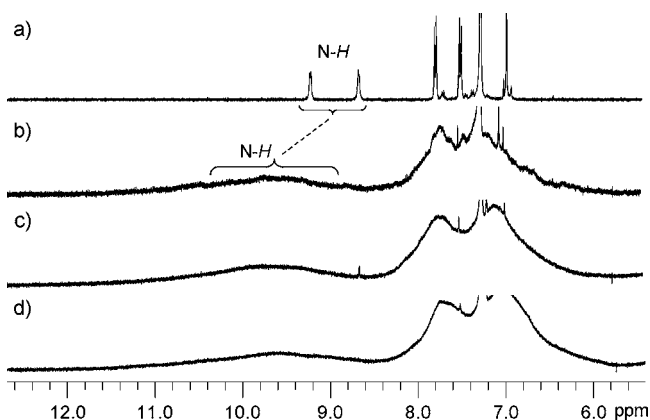


**Figure 1.** Partial  $^1\text{H}$  NMR spectra of (a) **4**, (b) **2a**, (c) **2b**, and (d) **3** in  $\text{CDCl}_3$  at 298 K. The concentration was 2.0 mM.

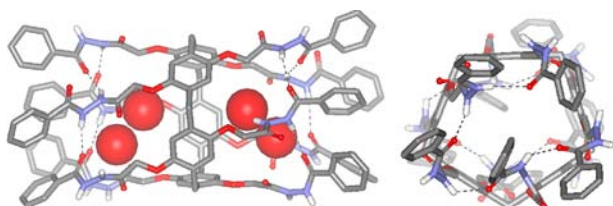


**Figure 2.** Crystal structure (stick model) of **2b**: (left) side view; (right) top view. The O atoms of four entrapped water molecules are highlighted using CPK models. The *tert*-butyl groups and H atoms on the C atoms have been omitted for clarity.

form eight intramolecular hydrogen bonds in a head-to-tail manner (Figure 2, left). Another two form intermolecular hydrogen bonds. However, the whole molecule produces a tubular cavity (Figure 2, right). In view of the dynamic nature of hydrogen bonding in solution, it is reasonable to assume that this series of pillar[5]arene derivatives should also form similar tubular conformations. The tubular cavity of **2b** also encapsulates four water molecules that are hydrogen-bonded with carboxylic groups (Figure 2, left). This observation prompted us to investigate the capacity of these molecules in transporting water across membranes.

The water transport property of the tubular structures across lipid bilayers was investigated using dynamic light scattering (DLS).<sup>15</sup> Large unilamellar vesicles in buffer containing NaCl (100 mM) were first prepared from egg yolk *L*- $\alpha$ -phosphatidylcholine (EYPC)<sup>16</sup> and then suspended in pure water to produce different osmotic pressures inside and outside the vesicles. Aliquots of DMSO solutions of **1**, **2a**, and **3** (0.3% molar ratio relative to lipid) were injected into the suspensions of the vesicles. The light scattering and vesicle diameters were then monitored for 400 min (Figure 3). For the systems containing **1** and **2a**, the normalized light scattering slowly decreased by 5 and 10%, respectively, after 400 min, while for the system containing **3**, the light scattering decreased by 25% after 125 min (Figure 3a). The decrease in light scattering is a result of swelling of the vesicles.<sup>9</sup> It is established that lipid membranes themselves allow only for slow transport of water.<sup>17</sup> A control experiment also showed that in the absence of the tubular compounds, a very slight light scattering decrease (2%) was observed (Figure 3a, black). Thus, the above light scattering decrease can be attributed to water transport from the outside to the inside of the vesicles that was realized through insertion of the tubular molecules into the membranes

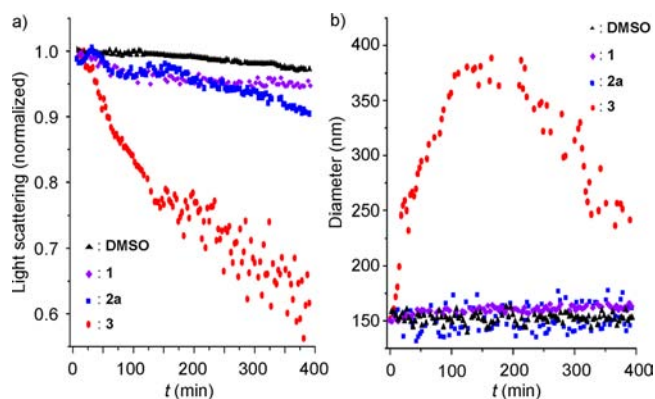


**Figure 3.** (a) Changes in light scattering and (b) mean diameter of the vesicles with time after addition of a DMSO solution of **1**, **2a**, or **3** (0.3 mol % relative to lipid) or pure DMSO. The vesicles were loaded with NaCl (100 mM) and suspended in distilled water.

and driven by the osmotic pressure difference between the outside and inside of the vesicles (Figure 4). The larger light scattering decrease caused by **3** suggests that it was more efficient than **1** and **2a** in transporting water. After 125 min, the light scattering decrease continued for **3** but showed larger fluctuations, probably due to precipitation of the very large vesicles.<sup>18</sup>

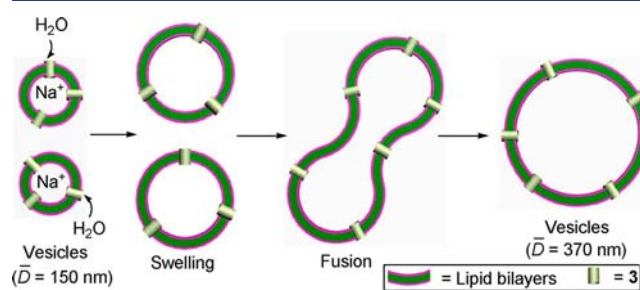


**Figure 4.** Schematic representation of the increase in vesicle size caused by **3**-mediated outside-to-inside water transport.

By fitting the above light scattering versus time plots with a linear model,<sup>9</sup> the water-transport activity rate constants ( $k$ ) for **1**, **2a**, and **3** were calculated to be  $(3.6 \pm 0.4) \times 10^{-7}$ ,  $(9.4 \pm 0.5) \times 10^{-7}$ , and  $(3.58 \pm 0.2) \times 10^{-5} \text{ s}^{-1}$ , respectively. The fact that **3a** displayed the highest transport activity may be rationalized by considering that its length (5.1 nm as determined using a CPK model) matches well the width of the lipid bilayer (5.0 nm).<sup>5b</sup> CPK modeling showed that tubular **2a** has a length of 3.5 nm. Thus, it might also transport water in a single-molecular manner that is less efficient because of possible blockage at the ends by lipid molecules. The even shorter compound **1** could mediate this process only through stacking of two molecules in the membrane<sup>12</sup> and thus was also less efficient.

Figure 3b shows that adding the solution of **1** or **2a** in DMSO caused a small increase in the mean diameter of the vesicles, while pure DMSO did not impose a detectable influence. In contrast, adding **3** caused the mean vesicle diameter to increase from ca. 150 to ca. 370 nm within 125 min. After that, the vesicle diameter decreased gradually, most likely because of the precipitation of large vesicles. The size of the vesicles increased 1.5-fold before 125 min, which exceeded the limitation of simple vesicle swelling (10%).<sup>19</sup> To get a deep

insight into the vesicle swelling process, the vesicle samples were checked by cryogenic scanning electron microscopy (cryo-SEM) (Figure 5), which indicated that the size of the

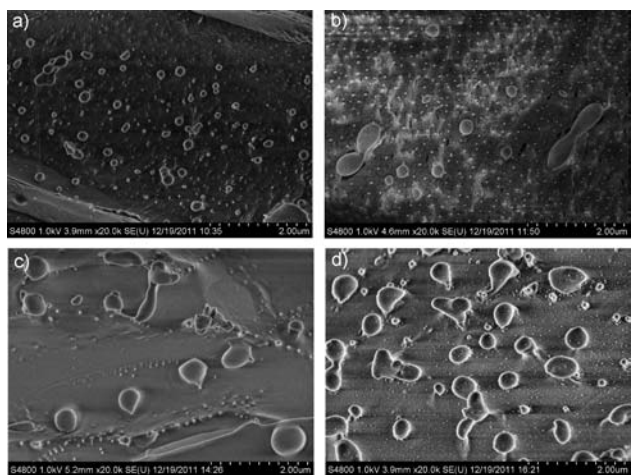


**Figure 5.** Cryo-SEM images of the sample recorded (a) 0, (b) 60, (c) 150, (d) 350 min after addition of **3** (0.3 mol % relative to lipid), highlighting the size increase of vesicles with time as well as vesicle fusion (b). The bright particles are ice crystals.

vesicles increased with time. Figure 5b also showed the fusion of vesicles, which may account for the formation of large vesicles. When the vesicles were suspended in buffer containing NaCl (100 mM), the osmotic pressure was the same inside and outside the vesicles. Adding **3** to the suspension did not cause the light scattering and size of the vesicles to change within 200 min (Figure S20 in the SI), implying that **3** did not promote the fusion of vesicles. Thus, the above fusion should be a result of vesicle swelling that occurred through the outside-to-inside water transport (Figure 4).<sup>20</sup>

The water transport activities of **1**, **2a** and **3** at different channel to lipid ratios (mol %) was further investigated. It was found that a high channel/lipid ratio (>0.9 mol %) caused the vesicles to break, affording precipitates in a few minutes. When the molar ratio was <0.09%, the transport constants of **1** and **2a** could not be obtained because of their weak transport ability. The transport activity of **3** was found to be linearly dependent on the molar ratio over the range 0.027–0.45% (Figure 6). This linear relationship supports the above single-molecular

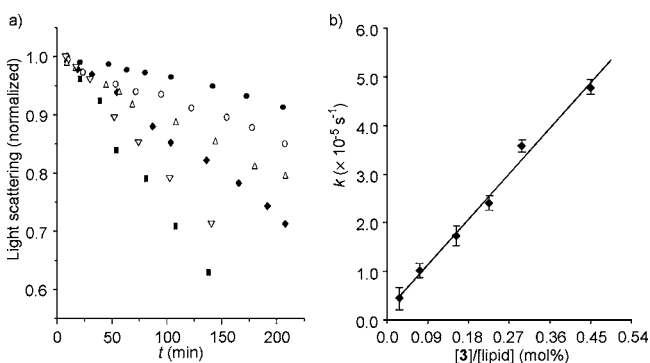


**Figure 6.** (a) Changes in light scattering with time in the presence of **3** [0.027% (●), 0.075% (○), 0.15% (△), 0.23% (◆), 0.3% (▽), and 0.45% (■) relative to lipid]. (b) Plot of the transport rate constant  $k$  for **3** against the molar ratio relative to lipid.

mechanism. The osmotic water permeability ( $P_f$ )<sup>21</sup> of **3** at 0.3 mol % was calculated to be  $8.6 \times 10^{-10} \text{ cm s}^{-1}$  (see the SI) by assuming that two vesicles fused to produce one big vesicle and that all of the added channel molecules were inserted into lipid bilayers. The actual value should be higher than this estimated one, since it is impossible for all of the molecules to be inserted into the membranes.

The selectivity of the channels for  $\text{OH}^-$  and  $\text{H}^+$  was also studied by imposing a pH gradient across the membranes of the vesicles. A suspension of vesicles entrapping the pH-sensitive dye 8-hydroxypyrene-1,3,6-trisulfonate (HPTS)<sup>22</sup> and  $\text{Na}^+$  buffer (pH 7.0 inside the vesicles) was prepared and then added to a  $\text{K}^+$  buffer having a pH of 7.6 to produce a higher  $\text{K}^+$  and  $\text{OH}^-$  concentration outside the vesicles. The  $\text{OH}^-$  flux through the membranes was assessed by monitoring the fluorescence intensity of HPTS. Adding **1**, **2a**, and **3** (0.3 mol % relative to lipid) to the above vesicle suspension caused a small change (<5%) in the fluorescence intensity (Figure 7a).

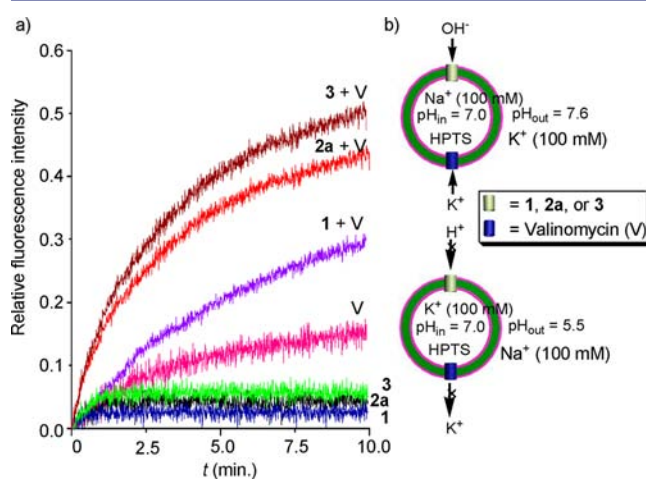


**Figure 7.** (a) Change in fluorescence intensity ( $\lambda_{\text{ex}} = 460 \text{ nm}$ ,  $\lambda_{\text{em}} = 510 \text{ nm}$ ) of vesicles with time after addition of **1**, **2a**, or **3** (0.3 mol % relative to lipid) and/or valinomycin (0.002 mol % relative to lipid). The vesicles were loaded with NaCl (100 mM) and HPTS (0.1 mM) buffered at pH 7.0 with HEPES (10 mM) and suspended in KCl (100 mM) solution (buffered to pH 7.6). (b) Schematic representation of (top)  $\text{OH}^-$  transport and (bottom)  $\text{H}^+$  blockage in the channels.

However, adding their mixtures with valinomycin (0.002 mol % relative to lipid), an efficient  $\text{K}^+$  carrier,<sup>23</sup> caused the intensity to increase by 28, 42, and 51%, respectively, in 10 min. In contrast, the same amount of valinomycin itself resulted in only a 13% increase in the fluorescence intensity. These results support the conclusion that **1**, **2a**, and **3** can also transport  $\text{OH}^-$  (Figure 7b, top). Again, **3** exhibited the highest transport ability, which can also be attributed to the fact that its length fits best with the width of the lipid bilayer. Using a similar strategy, we prepared a suspension of vesicles entrapping HPTS and  $\text{K}^+$  buffer (pH 7.0 inside the vesicles) and then added it to a  $\text{Na}^+$  buffer having a pH of 5.5 to produce higher  $\text{H}^+$  concentration outside the vesicles. In the presence or absence of valinomycin, **1**, **2a**, and **3** (0.3 mol % relative to lipid) did not cause any change in the fluorescence intensity of HPTS (Figure S21), suggesting that they did not transport  $\text{H}^+$  across the membrane (Figure 7b, bottom). This was not unexpected, as a flux of  $\text{H}^+$  has to be realized through a continuous hydrogen-bonding network formed by water or hydroxyl groups.<sup>12,24</sup> This result features one of the key functions of natural water channels,



which do not form the hydrogen-bonded water wires and thus block  $H^+$  flux.<sup>25</sup>

In conclusion, we have developed a class of artificial transmembrane water channels based on hydrazide-incorporated pillar[5]arenes. The pillar[5]arene derivatives are induced to form tubular conformations by intramolecular hydrogen bonding and thus can function as single-molecular channels to transport water across the lipid membrane at very low concentration. Although the transport rate is not as high as for natural channels, the results described here were obtained using unoptimized molecules. Currently we are modifying the backbones to achieve more efficient systems.

## ■ ASSOCIATED CONTENT

### ● Supporting Information

Synthetic procedures and characterization data for **1–4**; detailed procedures for water,  $OH^-$ , and  $H^+$  transport experiments; and a CIF file for **2b**. This material is available free of charge via the Internet at <http://pubs.acs.org>.

## ■ AUTHOR INFORMATION

### Corresponding Author

houjl@fudan.edu.cn

### Notes

The authors declare no competing financial interest.

## ■ ACKNOWLEDGMENTS

This work was supported by NSFC (20902012 and 91027008), FANEDD (200930), STCSM (10PJ1401200), the Innovation Program of SHMEC (10ZZ01), and Shanghai Key Laboratory of Molecular Catalysis and Functional Materials.

## ■ REFERENCES

- (1) Preston, G. M.; Carroll, T. P.; Guggino, W. B.; Agre, P. *Science* **1992**, *256*, 385.
- (2) de Groot, B. L.; Frigato, T.; Helms, V.; Grubmuller, H. *J. Mol. Biol.* **2003**, *333*, 279.
- (3) Agre, P.; King, L. S.; Yasui, M.; Guggino, W. B.; Ottersen, O. P.; Fujiyoshi, Y.; Engel, A.; Nielsen, S. *J. Physiol.* **2002**, *542*, 3.
- (4) (a) Kumar, M.; Grzelakowski, M.; Zilles, J.; Clark, M.; Meier, W. *Proc. Natl. Acad. Sci. U.S.A.* **2007**, *104*, 20719. (b) Kaufman, Y.; Berman, A.; Freger, V. *Langmuir* **2010**, *26*, 7388.
- (5) (a) Akerfeldt, K. S.; Lear, J. D.; Wasserman, Z. R.; Chung, L. A.; DeGrado, W. F. *Acc. Chem. Res.* **1993**, *26*, 191. (b) Gokel, G. W.; Mukhopadhyay, A. *Chem. Soc. Rev.* **2001**, *30*, 274. (c) Fyles, T. M. *Chem. Soc. Rev.* **2007**, *36*, 335. (d) Davis, A. P.; Sheppard, D. N.; Smith, B. D. *Chem. Soc. Rev.* **2007**, *36*, 348. (e) Matile, S.; Vargas Jentzsch, A.; Montenegro, J.; Fin, A. *Chem. Soc. Rev.* **2011**, *40*, 2453. (f) Gale, P. A. *Acc. Chem. Res.* **2011**, *44*, 216.
- (6) (a) Cho, H.; Widanapathirana, L.; Zhao, Y. *J. Am. Chem. Soc.* **2011**, *133*, 141. (b) Cho, H.; Zhao, Y. *Langmuir* **2011**, *27*, 4936. (c) Zhang, S.; Zhao, Y. *Chem.—Eur. J.* **2011**, *17*, 12444.
- (7) (a) Hummer, G.; Rasaiah, J. C.; Noworyta, J. P. *Nature* **2001**, *414*, 188. (b) Zhu, F.; Schulten, K. *Biophys. J.* **2003**, *85*, 236. (c) Striolo, A. *Nano Lett.* **2006**, *6*, 633.
- (8) (a) Engels, M.; Bashford, D.; Ghadiri, M. R. *J. Am. Chem. Soc.* **1995**, *117*, 9151. (b) Portella, G.; de Groot, B. L. *Biophys. J.* **2009**, *96*, 925. (c) Titov, A. V.; Wang, B.; Sint, K.; Kral, P. *J. Phys. Chem. B* **2010**, *114*, 1174. (d) Liu, J.; Fan, J.; Tang, M.; Cen, M.; Yan, J.; Liu, Z.; Zhou, W. *J. Phys. Chem. B* **2010**, *114*, 12183.
- (9) An example of a self-assembled imidazole-quartet water channel has been reported. See: Duc, Y. L.; Michau, M.; Gilles, A.; Gence, V.; Legrand, Y.-M.; Lee, A.; Tingry, S.; Barboiu, M. *Angew. Chem., Int. Ed.* **2011**, *50*, 11366.
- (10) Verkman, A. S. *J. Cell Sci.* **2011**, *124*, 2107.

(11) Si, W.; Hu, X.-B.; Liu, X.-H.; Fan, R.; Chen, Z.; Weng, L.; Hou, J.-L. *Tetrahedron Lett.* **2011**, *52*, 2484.

(12) Si, W.; Chen, L.; Hu, X.-B.; Tang, G.; Chen, Z.; Hou, J.-L.; Li, Z.-T. *Angew. Chem., Int. Ed.* **2011**, *50*, 12564.

(13) For the application of pillar[5]arene derivatives in molecular recognition, see: (a) Ogoshi, T.; Kanai, S.; Fujinami, S.; Yamagishi, T.-A.; Nakamoto, Y. *J. Am. Chem. Soc.* **2008**, *130*, 5022. (b) Li, C.; Xu, Q.; Li, J.; Yao, F.; Jia, X. *Org. Biomol. Chem.* **2010**, *8*, 1568. (c) Dong, S.; Luo, Y.; Yan, X.; Zheng, B.; Ding, X.; Yu, Y.; Ma, Z.; Zhao, Q.; Huang, F. *Angew. Chem., Int. Ed.* **2011**, *50*, 1397. (d) Hu, X.-B.; Chen, L.; Si, W.; Yu, Y.; Hou, J. *Chem. Commun.* **2011**, *47*, 4694. (e) Zhang, H.; Strutt, N. L.; Stoll, R. S.; Li, H.; Zhu, Z.; Stoddart, J. F. *Chem. Commun.* **2011**, *47*, 11420. (f) Cragg, P. J.; Sharma, K. *Chem. Soc. Rev.* **2012**, *41*, 597.

(14) Zhao, X.; Wang, X.-Z.; Jiang, X.-K.; Li, Z.-T.; Chen, G.-J. *J. Am. Chem. Soc.* **2003**, *125*, 15128.

(15) (a) Hallett, F. R.; Marsh, J.; Nickel, B. G.; Wood, J. M. *Biophys. J.* **1993**, *64*, 435. (b) Borgnia, M. J.; Kozano, D.; Calamita, G.; Maloney, P. C.; Agre, P. *J. Mol. Biol.* **1999**, *291*, 1169.

(16) Jeon, Y. J.; Kim, H.; Jon, S.; Selvapalam, N.; Oh, D. H.; Seo, I.; Park, C.; Jung, S. R.; Koh, D.; Kim, K. *J. Am. Chem. Soc.* **2004**, *126*, 15944.

(17) (a) Finkelstein, A.; Cass, A. *J. Gen. Physiol.* **1967**, *50*, 1765. (b) Andrasko, J.; Forsen, S. *Biochem. Biophys. Res. Commun.* **1974**, *60*, 813. (c) Lipschitz-Farber, C.; Degani, H. *Biochim. Biophys. Acta* **1980**, *600*, 291. (d) Huster, D.; Jin, A. J.; Arnold, K.; Gawrisch, K. *Biophys. J.* **1997**, *73*, 855.

(18) Sakai, N.; Matile, S. *Chirality* **2003**, *15*, 766.

(19) Haines, T. H.; Li, W.; Green, M.; Cummins, H. Z. *Biochemistry* **1987**, *26*, 5439.

(20) Cohen, F. S.; Akabas, M. H.; Finkelstein, A. *Science* **1982**, *217*, 458.

(21) Zhang, R.; Logee, K. A.; Verkman, K. S. *J. Biol. Chem.* **1990**, *265*, 15375.

(22) Kano, K.; Fendler, J. H. *Biochim. Biophys. Acta* **1978**, *509*, 289.

(23) Dobler, M. *Ionophores and Their Structures*; Wiley: New York, 1981.

(24) Weiss, L. A.; Sakai, N.; Ghebremariam, B.; Ni, C.; Matile, S. *J. Am. Chem. Soc.* **1997**, *119*, 12142.

(25) (a) Burykin, A.; Warshel, A. *Biophys. J.* **2003**, *85*, 3696. (b) Jensen, M.; Rothlisberger, U.; Rovira, C. *Biophys. J.* **2005**, *89*, 1744.